A class of slip-line field solutions for metal machining with elastic contact

K.P. Maity*, N.S. Das

Department of Mechanical Engineering, Regional Engineering College, Rourkela, Orissa 769-008, India

Abstract

The present investigation is concerned with a class of slip-line field solutions for metal machining involving chip curl. The solutions under consideration were first proposed by Kudo, who had found them to be statically inadmissible. In this study, these fields are analysed by assuming an elastic contact zone beyond the plastically stressed region. Force and moment equilibrium of the chip is realised by assuming the rigid chip to be acted upon by prescribed normal and shear forces in the elastic zone and by forces in the rigid–plastic boundary. Results are presented for variation in contact length, cutting force and thrust force, with variation in rake angle and interface friction conditions, both for power-law and exponential pressure distributions in the elastic contact zone

Keywords: Slip-line field solutions; Metal machining; Chip curl; Elastic contact

1. Introduction

A great deal of experimental work on metal machining has been performed in the last two decades to determine the distribution of stresses at the chip–tool interface by various investigators using different techniques. Photo-elastic [1,2], split tool [3,4], composite tool [5,6] and visioplasticity methods [7] have established that beyond the region of contact between a chip and a tool over which the chip is plastically stressed, there usually exists an extensive region of elastic contact. Further, the existence of elastic contact is known qualitatively from the observation that the contact length as obtained experimentally is much greater than the theoretical plastic contact length.

Even though the existence of an elastic contact region at the chip–tool interface has long been recognised experimentally, due emphasis of this feature has not been given in theoretical analysis of metal machining. The elastic zone in the contact length was first conjectured by Zorev [8], whilst Childs [9] proposed an approximate analysis with elastic contact using Dewhurst's slip-line field model [10] for free machining. He used the modified Dewhurst's field by replacing curved slip-line elements by circular arcs. He further observed that the theoretical results are closer to the experimental results when consideration is taken of the existence of an elastic contact region.

In the present investigation an attempt has been made to obtain slip-line field solutions with elastic contact for two different slip-line field models (Fig. 1(a) and Fig. 2(a)) as suggested by Kudo [11] for the case of machining with chip curl. Kudo observed that the above slip-line fields give kinematically admissible but statically inadmissible solutions for the above situation. Hence an alternative solution involving two convex slip-lines was proposed by the above author for one of the above solutions (Fig. 1), so that both the statical and kinematical requirements are satisfied. However, with the above modification, the normal stress at the chip–tool interface was found to decrease from the chip-releasing point to the tool tip, which is contrary to the actual distribution as observed in experimental investigations. With assumption of an elastic contact, it is possible to obtain viable statically and kinematically admissible solutions for the above two fields. The analysis has been carried out with the assumption of power-law and exponential distributions of the normal stresses in the elastic zone with coulomb friction. The cutting forces, chip reduction co-efficient, and radii of curvature of the chip with other parameters are

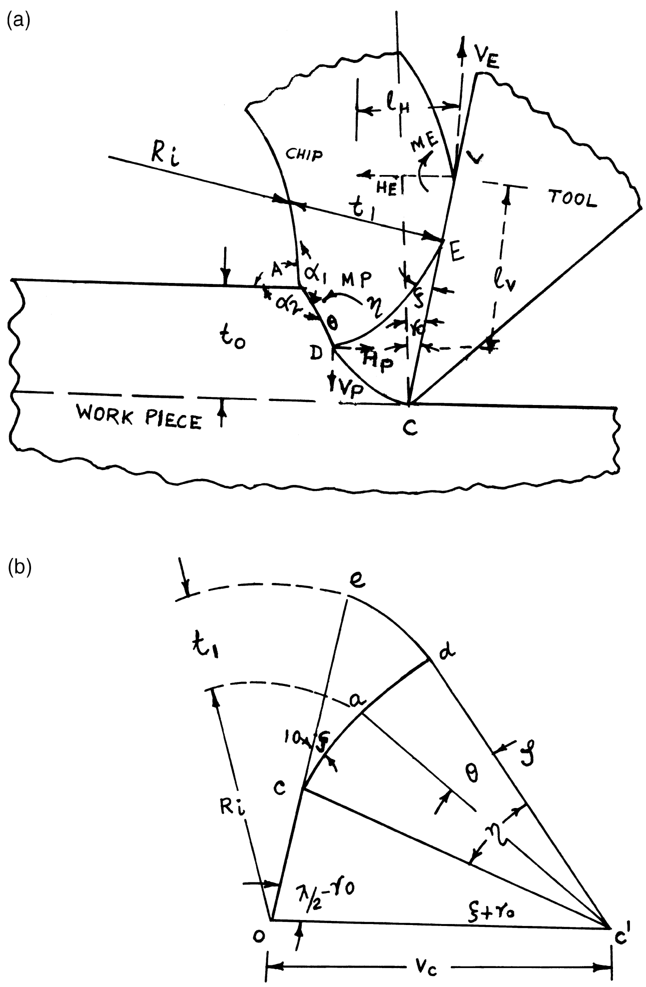

Fig. 1. Presenting: (a) the slip-line field model; and (b) the hodograph, for the first solution of Kudo [11].

estimated for different tool-geometry and cutting conditions. The variations of contact lengths with rake angles, friction at the chip–tool interface, exponents of the stress distribution in the elastic zone and the undeformed chip thickness are determined. The distribution of stresses in the plastic and elastic zone are also predicted.

It must be emphasised that slip-line field analysis does not take into account the elastic distribution of stresses. Further as pointed out by Childs [9], the introduction of an elastic zone marginally violates the mass continuity condition. However, despite these limitations, the present results are expected to be of value in metal cutting research.

2. Methodology

Two slip-line fields due to Kudo [11] for metal machining with chip curl are shown in Figs. 1 and 2 with their associated hodographs.

Referring to Fig. 1(a) it may seen that the curve ADC defines the primary shear line. The rigid–plastic boundary

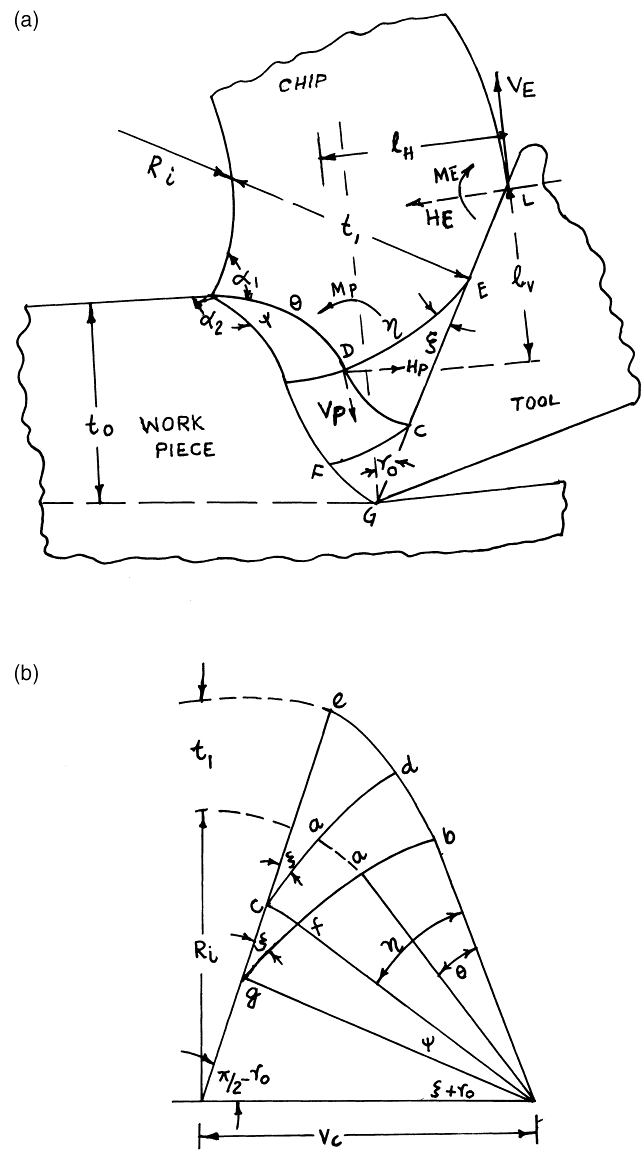

separating the chip from the plastically deforming region is indicated by EDA, where ED is the concave α-line and AD is the convex β-line. ECD is the plastically deforming material in contact with the tool. Thus, EC is the zone of plastic contact or the secondary shear zone. Since frictional shear traction in the plastically deforming region is assumed constant (τ=mk), slip-lines ED and CD meet the tool face at constant angles of ξ (=(1/2) $\cos^{-1}$m) and (π/2−ξ), respectively. As shown in Fig. 1(a), the material, after leaving the deforming region, undergoes rigid-body rotation, forming a curled chip of constant curvature.

Referring to the hodograph (Fig. 1(b)), it may be seen that the material suffers a velocity discontinuity of magnitude ρ on crossing the primary shear line. Thus, the velocity along the slip-line CDA is given by the circular arc cd and along the slip-line DE by the hodograph curve de. Since the chip is rotating rigidly with angular velocity ω, the lines DA and DE must also appear in the hodograph, but rotated through 90 degrees in the direction of ω and multiplied by the scale factor ω, i.e., ade must be geometrically similar to ADE [15]. Hence, slip-line DA is also a circular arc of radius ρ/ω.

The column vectors δ for the radius of curvature of the slip-line ED is calculated readily from the relationship:

$$\delta = (\rho/\omega)\ G\xi\eta c, \tag{1}$$

where G is the straight rough boundary operator as defined in [10] and c is a column vector representing a unit circle.

The second slip-line field shown in Fig. 2(a) is very similar to that given in Fig. 1(a) except that a singular field ACF is now interposed between the chip and the work material with another plastically deforming region CFG in contact with the tool face. Referring to the hodograph (Fig. 2(a)) it may be seen that gb is a circular arc of radius ρ.

Let δ_1 and δ_2 denote the column vectors in the power-series expansion of the radius of curvature of the slip-lines ED and AD, respectively. δ_1 is calculated from the circular arc gb using the relationship:

$$\delta_1 = (\rho/\omega) \quad G_{\xi\beta}c, \tag{2a}$$

where $\beta = \eta+\psi$.

AD in this case, however, is not part of a circular arc. Its radius of curvature is calculated from the equation:

$$\delta_2 = (\rho/\omega)S_{\sim}G^{-1}_{\xi\eta}G_{\beta\xi}c \tag{2b}$$

where $\sim = \eta-\theta$.

It may be noted that in both of these fields, the chip boundary is defined by three field variables: the angular range η of the α-line ED, the angular range θ of the β-line AD and the hydrostatic pressure P_E at E. As reported by Kudo [11], however, these three variables alone are not sufficient to ensure the force and moment equilibrium of the chip. Kudo therefore modified the slip-line field of Fig. 1(a) whereby the concave α-line was replaced by a convex line geometrically similar to the β-line AD. With this modification, static admissibility of the solution was satisfied, but the normal pressure increased from the tool tip to the chip separation point.

In the present analysis, the "force free" condition of the chip is realised by imposing externally the forces H_E and V_E

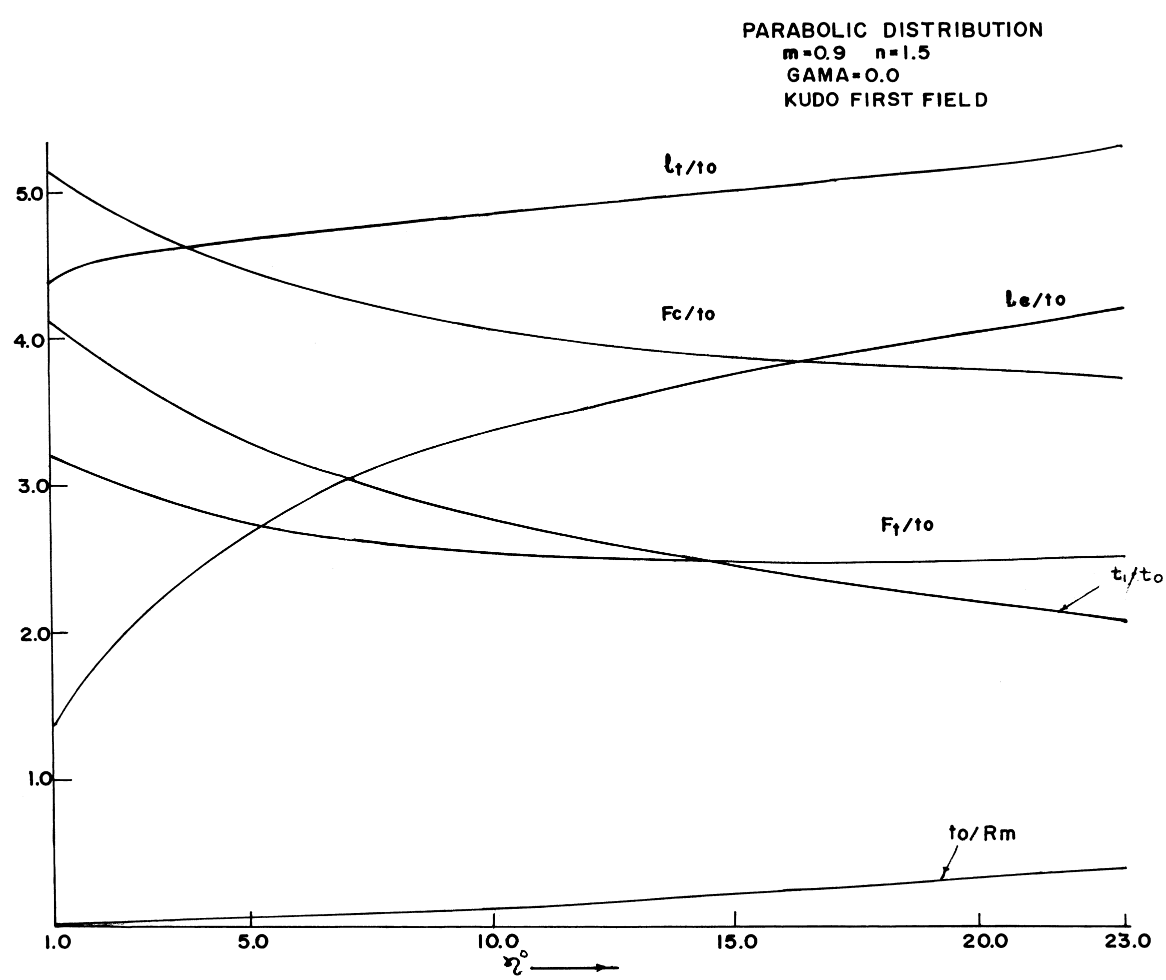

on the chip in the elastic contact length. The procedure is similar to that proposed by Childs [7]. For any given pressure distribution in the elastic contact length, H_E, V_E and elastic moment M_E are calculated readily (Appendix A). For equilibrium of the chip, these, together with the forces H_P and V_P and moment M_P in the chip boundary ADE, must simultaneously be equal to zero. Mathematically, this condition may be stated as:

$$F_1 = H_P - H_E = 0, \tag{3a}$$

$$F_2 = V_P - V_E = 0, \tag{3b}$$

$$F_3 = M_P - M_E + H_E L_H + V_E L_V = 0. \tag{3c}$$

A Fortran programme developed for analysing the above fields was used to calculate the radius of curvature of the slip-lines and the forces H_P and V_P and moment M_P in the chip boundary using the sub-routines given in [12]. For any given value of η and pressure distribution in the elastic contact zone (parabolic or exponential), the programme solves the above set of non-linear algebraic equations (3) with the help of an algorithm developed by Powell [13]. A "force-free" chip was assumed to be achieved when the values of θ P_E and X (to ratio of the elastic to the plastic contact length) computed in the above manner satisfied the inequality:

$$F_1^2 + F_2^2 + F_3^2 \leq 10^{-10}.$$

The programme then used the values of the optimised field variables to compute the machining parameters such as the uncut chip thickness, the cutting ratio, the curl radius, and the cutting and thrust forces. It also contained checks to determine whether the rigid vertices at A were over-stressed [16]. All of the programmes were run on an ALPHA DEC SERVER, the time required for each calculation being less than 1 s.

3. Results and discussion

The results of variations of different machining parameters with respect to field angle η from the present

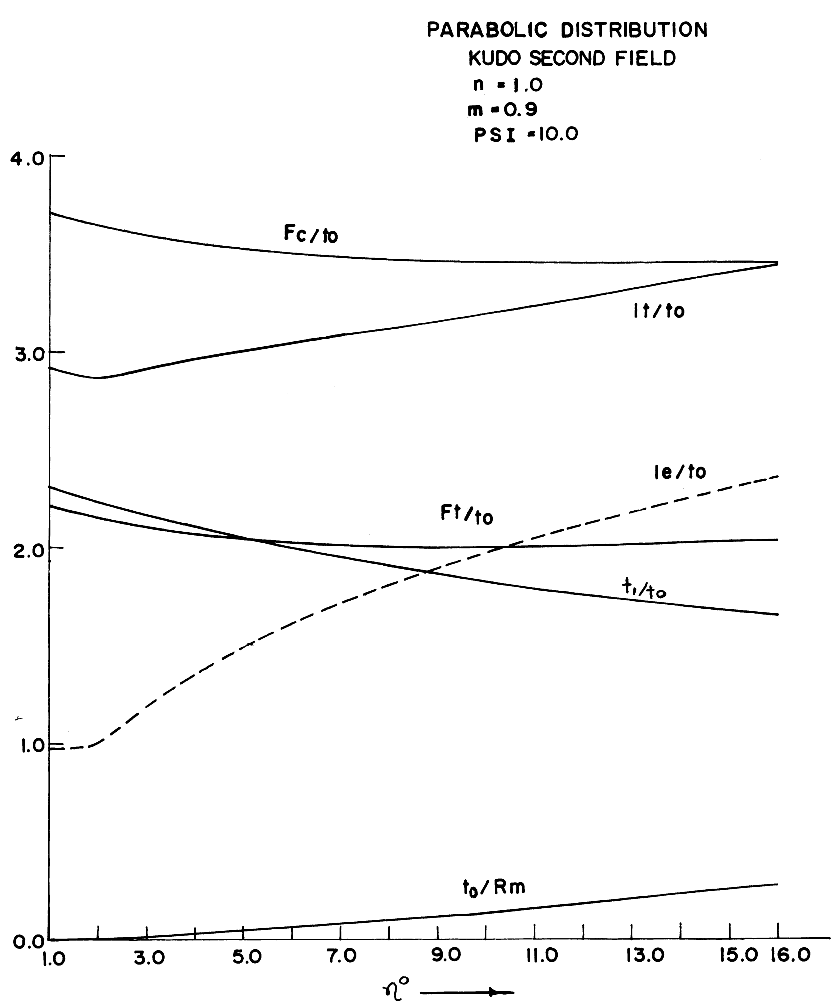

investigation are presented in Figs. 3 and 4 for a power-law as well as an exponential distribution of normal stresses in the elastic zone, respectively. The total contact length and elastic contact length per unit undeformed chip thickness increase with increase in the η value, whereas the cutting force, the thrust force per unit undeformed chip thickness, the chip reduction co-efficient and the mean radius of curvature per unit undeformed chip thickness decrease for both types of distributions of normal stresses. Similar solutions are also obtained for other rake angles, ranging from 0° to 15° using different exponents of distribution of normal stress in the elastic zone, both for the use of the power-law and the exponential distribution.

Fig. 5 gives the trend of variation of the maximum-total contact length as well as the maximum elastic contact per unit undeformed chip thickness with rake angle and exponents of distribution of normal stress. Both the total natural contact length as well as the elastic contact length decrease with increase in the rake angle, but increase with increase in the exponents of distribution. It is evident from Figs. 2 and 3 that the elastic contact length reduces with decrease in field angle η. When η is zero, Kudo's first slip-line field (Fig. 1) reduces to slip-line field model as suggested by Lee and Shaffer [14], which is valid only for the chip-streaming case, when there is no strain-hardening effect (Appendix B). Thus the minimum contact length is the only plastic contact at the chip–tool interface, as given by the Lee–Shaffer slip-line field model.

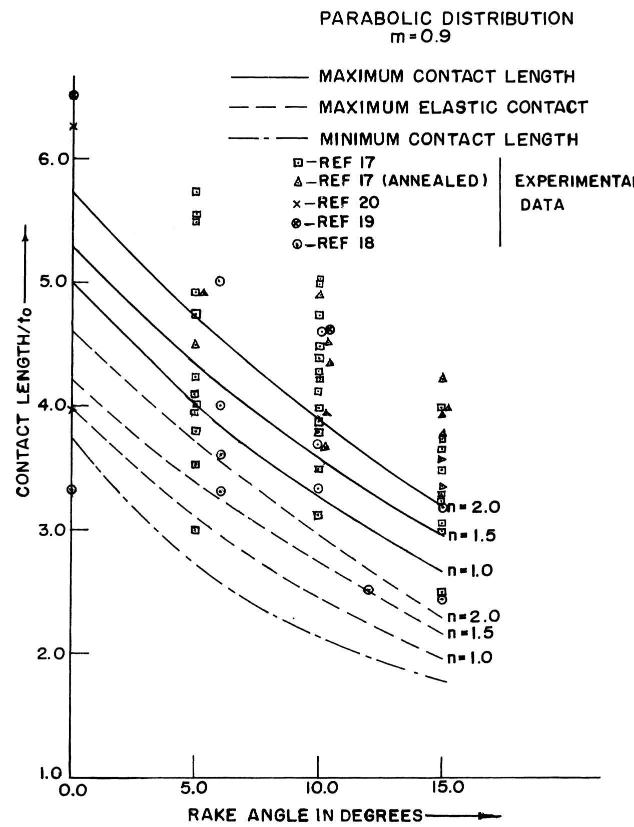

Fig. 5. The variation of maximum total contact length and maximum elastic contact length per unit undeformed chip thickness and exponents of distribution of normal stress.

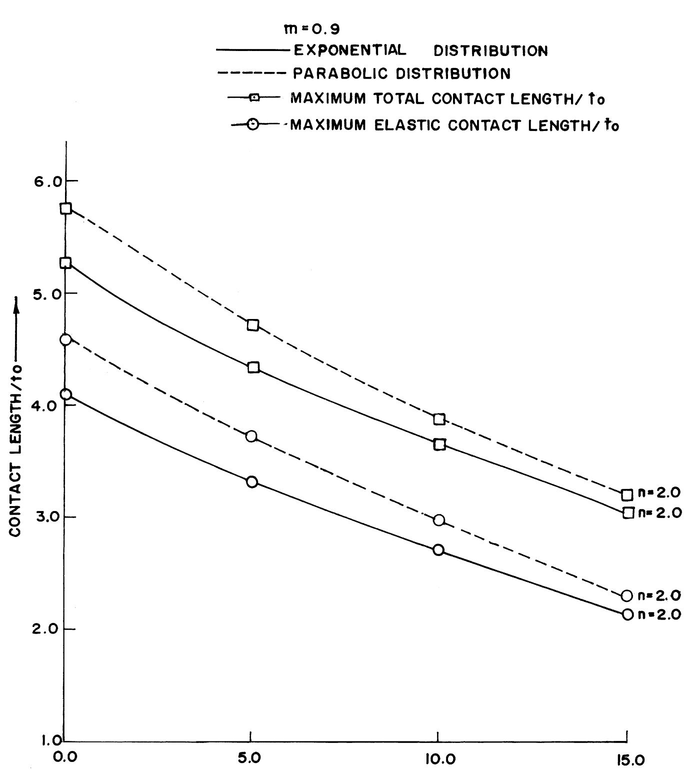

Fig. 6 indicates that both total contact length and the elastic contact length per unit undeformed chip thickness are greater for the case of the power-law distribution of normal stress than that of the exponential distribution in the elastic zone.

Fig. 7 gives a comparison of total contact length per unit undeformed chip thickness as obtained from the first and the second field. It is observed that total contact length per unit undeformed chip thickness increases with decrease in the field angle ψ. When ψ is zero, Kudo's second field reduces to the first field and the total contact length becomes maximum.

In Figs. 5 and 7 the tool–chip contact length values calculated from the present theoretical analysis are compared with experimental result as reported by Eggleston et al. [17], Chiffre [18], Usui et al. [19] and Pearce and Richardson [20]. In [17], the tool–chip contact length refers to the mark left by a streaming chip on the face as measured by a tool-maker's microscope. Chiffre [18], Usui et al. [19] and Pearce and Richardson [20] carried out experiments on restricted contact tools, the tool–chip contact length from these sources referring to the maximum restricted contact length beyond which the cutting forces remained sensibly constant.

Referring to Fig. 5, it may be seen that a better agreement between theory and experiment for steel may be obtained if a greater value of the power law exponent "n" is used. Similarly, a greater value of "ψ" would give a better correlation between theory and experiment for aluminium (Fig. 7).

It must be emphasised, however, that metal machining is a "non-unique" process and a great deal of scatter in the results is observed even under seemingly consistent experimental conditions.

Fig. 8 indicates the decrease in total contact per unit underformed chip thickness with decrease in friction at

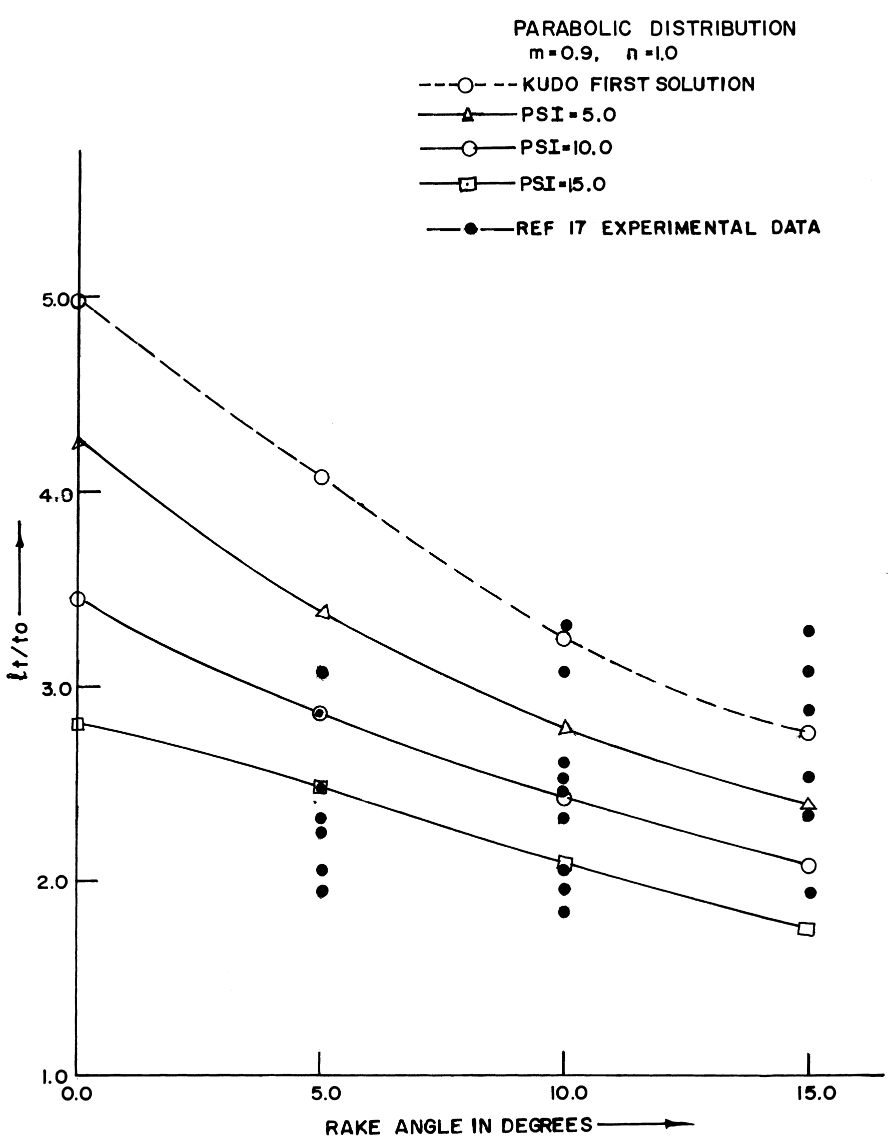

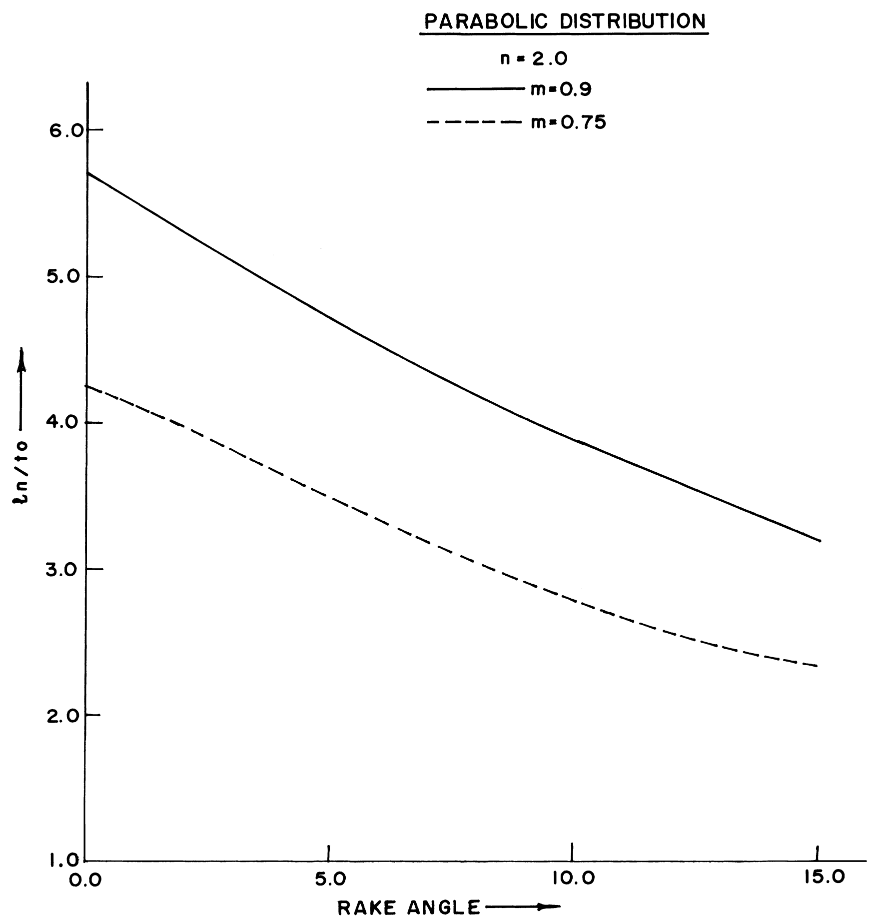

Fig. 8. As for Fig. 7 but for different levels of friction.

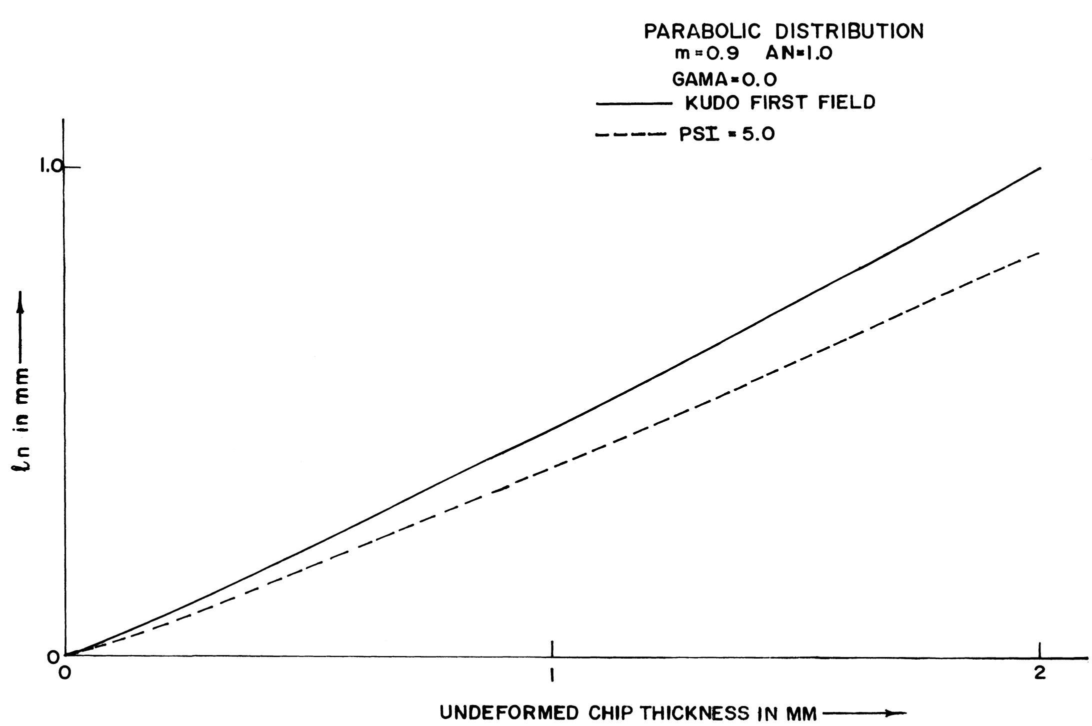

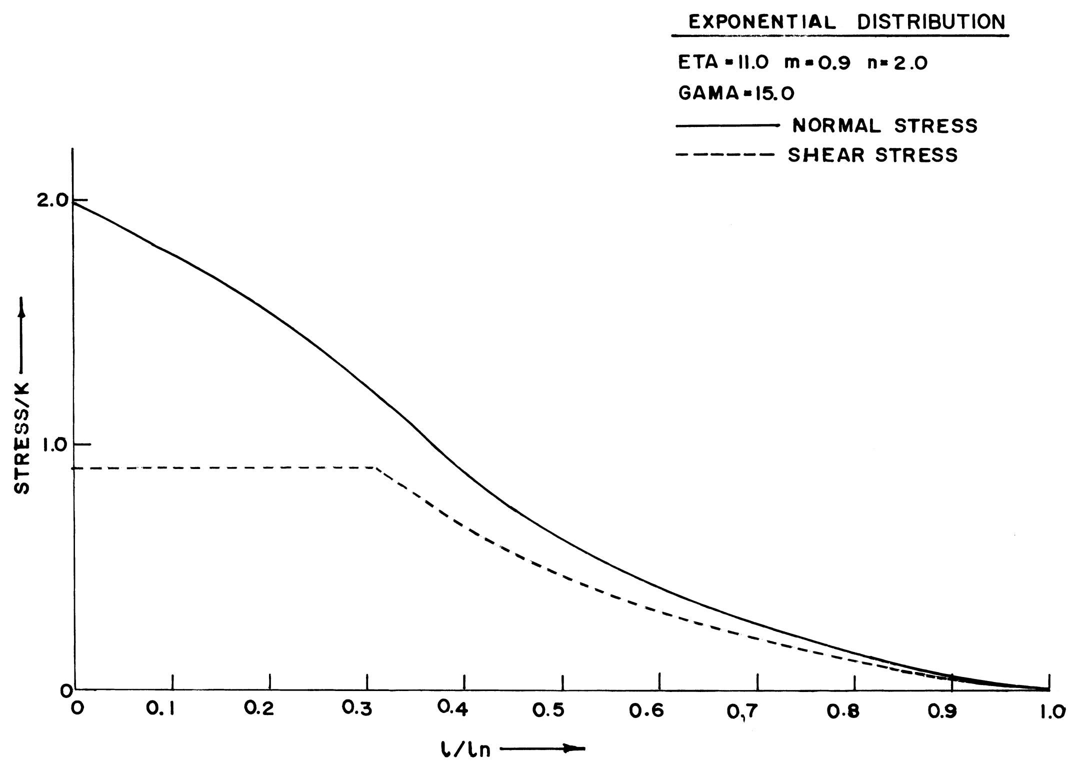

the chip–tool interface. The contact length increases with increase in undeformed chip thickness, as indicated in Fig. 9.

A typical distribution of normal stress and shear stress in the elastic and plastic zone for a rake angle equal to 15° are indicated in Fig. 10.

The shear stress, equal to 0.9 k, remains constant in the plastic zone, reducing gradually to zero at the chip-releasing point, whereas the normal stress increases from the minimum (zero) value at the chip- releasing point to a maximum value equal to 2.0 k at the tool tip. The trend of stress distribution is in agreement with the experimental observations reported earlier. Similar stress distributions are obtained also for other rake angles under different conditions.

4. Conclusions

1. Certain slip-line field models for free-machining as proposed by Kudo do not have a statically admissible solution for the case of chip curling. It is possible to obtain statically as well as kinematically admissible solutions for the above fields with the assumption of an elastic zone at the chip–tool interface.
2. Theoretically, there is no elastic contact length for the chip-streaming case, when there is no strain-hardening effect.
3. The total natural contact length as well as elastic contact length increase with increase in the index of distribution of normal stress, friction at the chip–tool interface, as well as the undeformed chip thickness, but decrease with increase in the rake angle.
4. Experimental data are found to be compatible with the total contact length obtained from theory. However, it is observed that a proper choice of the exponent of the distribution of normal stress gives the best comparison.

5. Nomenclature

K	yield stress in shear
L_e	elastic contact length
L_n	natural contact length
m_1	strain-hardening factor
m	constant-friction factor
n	exponent of the distribution of normal stress in the elastic zone
R_m	mean radius of curvature of the chip
t_0	undeformed chip thickness
t_1	chip thickness
V_c	cutting speed
P_E	hydrostatic pressure at E in slip-line ED
X	ratio of the elastic to the plastic contact length
F_C	tangential cutting force
F_t	thrust force
H_E, V_E	components of force in the elastic zone

Greek letters

θ, η, ψ	slip-line field angles
γ_0	orthogonal rake angle
δ_n	normal stress
μ	co-efficient of friction

Appendix A

Force analysis in the elastic contact zone

A.1 Power-law distribution of normal stress

The tool–chip separation point is taken as the origin. The normal stress on the tool at a distance 1 from the origin may be written as

$$\delta_N = \delta_E (1/1_e)^n,$$

where δ_E is the normal stress at the end point of plastic contact and l_e is the length of elastic contact. Thus the normal force F_N on the tool face at the elastic contact zone is:

$$F_N = \int_o^{l_e} \delta_N d1 = \delta_E l_e / n + 1.$$

A.1.1. Friction force at the elastic zone

$F_\tau = \mu \delta_E l_e / n + 1$ where $\mu = (P_E + \sin 2\xi)/\cos 2\xi$.

The moment about the tool–chip separation point is:

$$M_E = \delta_E l_e^2 / n + 2.$$

A.2 Exponential distribution of normal stresses

$$\delta_N = \delta_E (1 - e^{nl}/l_e)/(1 - e^n),$$

where n is the exponential index and l_e is the elastic contact length

$$F_N = \int_o^{l_e} \delta \, dl = \delta_E l_e (1 - e^n/n + 1/n)/(1 - e^n),$$

$$F_\tau = \mu F_N,$$

$$M_E = \delta_E l_e^2 ((1/2) - e^n/n + e^n/n^2 - 1/n^2)/(1 - e^n).$$

For the above two types of distribution of normal stress, the horizontal and vertical forces acting on the chip in the elastic zone are given as follows:

$$H_E = F_N \cos \gamma_0 + F_\tau \sin \gamma_0$$

$$V_E = F_N \sin \gamma_0 - F_\tau \cos \gamma_0.$$

Appendix B

For the chip-streaming case, Kudo's first field [11] is reduced to the slip-line field model as given by Lee and Shaffer [14] (Fig. 11). The angle made by the α -line at DE is given by $\xi = 1/2 \cos^{-1}(m)$, where m is the constant friction factor. Because of strain hardening, the hydrostatic pressure (p_1) and the yield shear stress (K_1) on the tool face become different from those (p,K) on the slip line AC. Let $p_1 = m_1 p$ and $k_1 = m_1 k$, where m_1 is the strain-hardening factor. Assuming a power-law distribution of normal stress in the elastic zone, the equilibrium of forces normal and along the chip–tool interface and the moment about the tool tip yield the following equations:

$$(p' \sin \xi + \cos \xi) = m_1 (p' + \sin 2\xi)(1 + x/n + 1), \quad \text{(B.1)}$$

$$pa \cos \xi - ka \sin \xi = k \cos 2\xi b + k \cos 2\xi \cdot xb/n + 1, \quad \text{(B.2)}$$

$$p'/2 = m_1 (p' + \sin 2\xi)[y^2/2 + y^2 x(1 + x)/n + 1 - x^2 y^2/n + 2], \quad \text{(B.3)}$$

where $Y = b/a$, $p' = p/k$ and $x = l_e/b$.

These equations are solved for unknown parameters y, p' and x to give:

$$y = 1/(m_1(1 + x/n + 1)(\cos \xi + \sin \xi)),$$

$$p' = 1,$$

$$X^2[m_1(n+2) - 2(n+1)] + X[2m_1(n+1)(n+2) - 2(n+1)(n+2)] + [m_1(n+1)^2(n+2) - (n+1)^2 - (n+1)^2(n+2)] = 0.0.$$

The above quadratic equation may be solved to determine the value of X. It may be noted that X becomes equal to zero when $m_1 = 1$. This indicates that elastic contact does not exist when there is no strain hardening for the chip-streaming case.

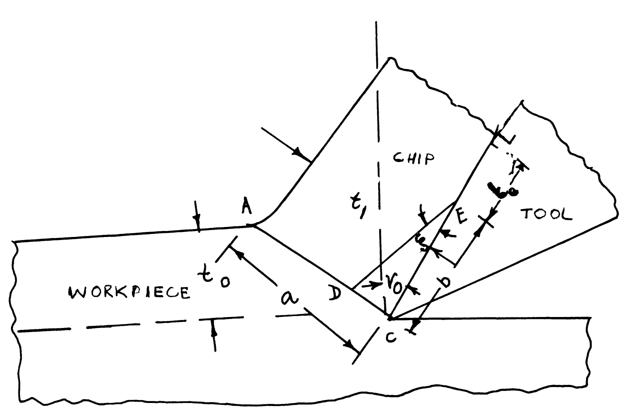

References

[1] H. Chandrasekaran, D.V. Kapoor, Trans. ASME, J. Eng. Ind. 87 (1965) 495–502.
[2] E. Usui, H. Takeyama, Trans. ASME, J. Eng. Ind. 82 (1960) 303.
[3] T.H.C. Childs, M.I. Mahdi, Ann. CIRP 38 (1989) 55–58.
[4] G. Barrow, W. Graham, T. Kurimoto, Y.F. Leong, Int. J. Mach. Tool Des. Res. 22(1) (1982) 75–85.
[5] S. Kato, K. Yamaguchi, M. Yanda, Trans. ASME, J. Eng. Ind. 94 (1972) 683–689.
[6] L.C. Lee, X.D. Liu, K.Y. Lam, Int. J. Mach. Tools Manufact. 35 (1995) 373–382.
[7] T.H.C. Childs, Proc. I. Mech. E. London 186 (1973) 717–727.
[8] N.N. Zorev, ASME Proc. Conf. Int. Res. Prod. Eng. New York 85 (1963) 42–49.
[9] T.H.C. Childs, Int. J. Mech. Sci. 22 (1980) 457–466.
[10] P. Dewhurst, Proc. Roy. Soc. London A 360 (1978) 587–610.
[11] H. Kudo, Int. J. Mech. Sci. 7 (1965) 43–55.
[12] P. Dewhurst, I.F. Collins, Int. J. Numer. Meth. Eng. 7 (1973) 357–378.
[13] J.L. Kuester, J.H. Mize, Optimisation Techniques with Fortran, McGraw-Hill, New York, 1973.
[14] E.h. Lee, B.W. Shaffer, J. Appl. Mech. 18 (1951) 405.
[15] A.P. Green, J. Mech. Phys. Solids 9 (73) (1954).
[16] R. Hill, J. Mech. Phys. (1954) 278–285.
[17] D.M. Eggleston, R. Herzog, E.G. Thomsen, Trans. ASME B81 (1959) 263–279.
[18] L. De Chiffre, Int. J. Mech. Tool Des. Res. 22(4) (1982) 321–332.
[19] E. Usui, K. Kikuchi, K. Hoshi, Trans. ASME B86 (1964) 95–104.
[20] D.F. Pearce, D.B. Richardson, Int. J. Prod. Res. 13(1) (1975) 75–82.